Chemistry and Physics of Lipids 224 (2019) 104726

Contents lists available at ScienceDirect

Chemistry and Physics of Lipids

journal homepage: www.elsevier.com/locate/chemphyslip

Effect of surface charge on the size-dependent cellular internalization of liposomes

Kumiko Sakai-Kato*, Kohki Yoshida, Ken-ichi Izutsu

Division of Drugs, National Institute of Health Sciences, 3-25-26 Tonomachi, Kawasaki-ku, Kawasaki, Kanagawa, 210-9501, Japan

ARTICLE INFO

Keywords:
Liposome
Size dependence
Surface charge
Lipid composition
Internalization

ABSTRACT

Here we report that the size dependence of cellular internalization of liposomes differs depending on the surface charge. We prepared liposomes of various lipid compositions ranging from 100 to 200 nm size. It was found that cationic liposomes composed of 1,2-Dioleoyl-sn-glycero-3-phosphocholine (DOPC) and 1,2-Dioleoyl-3-trimethylammonium-propane (DOTAP) were most effectively internalized into cells when their mean particle sizes were around 180 nm. When their size was reduced to around 90 nm, the level of internalization reduced six-fold. Conversely, hydrogenated soy phosphatidylcholine (HSPC)/*N*-(carbonyl-methoxypolyethylene glycol 2000)-1,2-distearoyl-sn-glycero-3-phosphoethanolamine (PEG2000-DSPE)/cholesterol(Chol) liposomes, HSPC/PEG2000-DSPE liposomes, and HSPC/Chol liposomes were most readily internalized when they were around 110 to 130 nm in mean particle size. Unlike DOPC/DOTAP liposomes the difference between the maximum and minimum levels of internalization was less than two-fold. It has been suggested that strong electrostatic interactions between cationic liposomes and the negatively charged plasma membrane affect the size dependence and optimal size range for internalization of liposomes. Size dependence of internalization should be carefully monitored for effective formulation development and quality control of liposome drug products.

1. Introduction

Recently, oligonucleotides such as RNA or DNA have attracted attention as new modalities for drug development (Dowdy, 2017). Because the targets of these drugs are typically found in subcellular locations, it is necessary to employ a carrier to transport the drugs into the target cells. Furthermore, around 60% of total expressed proteins are soluble proteins (Uhlén et al., 2015), making it essential that drug candidates – including nucleic acid or peptide drugs – are developed toward these intracellular targets (Ahlbach et al., 2015). In addition to the chemical modification of drugs (Khvorova and Watts, 2017), the use of nanoparticles as drug carriers into cells is a very promising avenue for advancing the delivery of therapeutics (Ferrari, 2005). Lipid nanoparticles, especially liposomes, are one of the most popular potential carrier nanoparticles (Barenholz, 2012). Selecting the appropriate lipids (e.g. head group and chain length), compositions, and surface modifications to achieve the desired performance (for example, targeting, drug release, or stability) of the product is often challenging task. During drug formulation studies and quality control, it is also important to clarify the critical physicochemical properties in terms of their interaction with cells or proteins in vivo and pharmacokinetics of the liposome drug products, to ensure optimal efficacy and safety of drug products (Ehmann et al., 2013; Sakai-Kato et al., 2015). In the case of liposomes, size is reported to be one of the most important properties affecting the efficacy and safety of the drug products (Sahay et al., 2010).

Several studies have reported the relationship between size and cellular internalization of nanoparticles (Sahay et al., 2010; Zhang et al., 2015). However, because of the complex interaction of nanoparticles with the plasma membrane, there are various mechanisms involved in the internalization of nanoparticles, such as endocytosis through clathrin-dependent or non-specific interactions (Zhang et al., 2015). It is therefore anticipated that the optimal size of liposomes will vary depending on other physicochemical properties of the particles. Although these properties can be tuned by altering the lipid composition, there are no reports relating the size dependence of internalization to other physicochemical properties.

The present study sought to elucidate the influences of the physicochemical properties of liposomes on their size-dependent cellular internalization. This information would enable rational design of nanoparticle formulations and improve quality control. Surface charge and liposome size are two major variables potentially affecting the cellular internalization of liposomes, and so a possible contribution of these variables to the internalization mechanisms is discussed.

* Corresponding author.
E-mail address: kumikato@nihs.go.jp (K. Sakai-Kato).

https://doi.org/10.1016/j.chemphyslip.2019.01.004
Received 11 July 2018; Received in revised form 9 October 2018; Accepted 16 January 2019
Available online 17 January 2019

2. Materials and methods

2.1. Materials and cells

Hydrogenated soy phosphatidylcholine (HSPC), *N*-(carbonyl-methoxypolyethylene glycol 2000)-1,2-distearoyl-sn-glycero-3-phosphoethanolamine (PEG2000-DSPE), and 1,2-Dioleoyl-sn-glycero-3-phosphocholine (DOPC) were purchased from NOF Corporation (Tokyo, Japan); 25-[*N*-[(7-nitro-2-1,3-benzoxadiazol-4-yl)methyl] amino]-27-norcholesterol (NBD-Chol), 1,2-Distearoyl-sn-glycero-3-phosphoethanolamine-*N*-[poly(ethylene glycol)2000-*N*′-carboxy-fluorescein] (ammonium salt) (PEG2000-PE-CF), 1-Oleoyl-2-[12-[(7-nitro-2-1,3-benzoxadiazol-4-yl)amino]dodecanoyl]-sn-glycero-3-phosphocholine (NBD-DOPC), and 1,2-Dioleoyl-3-trimethylammonium-propane (Chloride Salt) (DOTAP) were purchased from Avanti Polar Lipids (Alabaster, AL, USA); Dulbecco's Modified Eagle medium (DMEM) were purchased from Life Technologies (Brooklyn, NY, USA). Fetal bovine serum (FBS) was obtained from Nichirei Biosciences (Tokyo, Japan). All other chemicals used in this study were of the highest purity available. HepG2 cells (American Type Culture Collection, Manassas, VA, USA) were cultured in DMEM supplemented with 10% FBS and 100 U/mL penicillin–streptomycin. Cells were grown in a humidified incubator at 37 °C and 5% CO_2.

2.2. Preparation of liposomes

The lipid composition of the liposomes used in our experiments were: HSPC/PEG2000-DSPE/Chol/NBD-Chol (56.3/5.3/38.4/1 mol %), HSPC/PEG2000-DSPE/Chol/PEG2000-PE-CF (56.3/4.3/38.4/1 mol %), HSPC/PEG-DSPE/NBD-Chol (94.7/5.3/1 mol %), HSPC/Chol/NBD-Chol (60/39/1 mol %), and DOPC/DOTAP/NBD-DOPC (49/50/1 mol %). These liposomes were prepared using a modified Bangham method (Bangham et al., 1965). Briefly, the desired amounts of lipids were mixed in chloroform, and the mixture was dried by evaporation at 60 °C to create a thin homogeneous lipid film. The film was further dried overnight under vacuum desiccation to remove residual solvent. In the case of HSPC/PEG2000-DSPE/Chol and HSPC/PEG2000-DSPE liposomes, the dried film was hydrated with 2 mL of 5% (w/w) aqueous glucose solution under mechanical agitation at 70 °C for 5–10 min. The hydrated lipid solution was dispersed by sonication for 3 min in a bath-type sonicator (AS ONE, Tokyo, Japan). The dispersion was passed through a Mini-extruder (Avanti Polar Lipids) equipped with a 400 nm polycarbonate filter 21 times. For the preparation of liposomes with various sizes, extrusion through a 200 nm, 100 nm, or 50 nm polycarbonate filter was combined with further downsizing by a tip-type sonicator (Sonics, Newtown, CT, USA), depending on the intended size. In the case of HSPC/Chol liposomes, the lipid solutions were hydrated with 2 mL of 5% (w/w) aqueous glucose solution at 70 °C in a water bath, then freeze-thawed five times. The dispersion was passed through a Mini-extruder equipped with a 200 nm polycarbonate filter 21 times, then dispersed by a tip-type sonicator. In case of DOPC/DOTAP liposomes, the lipid solutions were hydrated with 2 mL of 5% (w/w) aqueous glucose solution at 50 °C in a water bath, then freeze-thawed five times. The dispersion was passed through a Mini-extruder equipped with a 400 nm polycarbonate filter 21 times, followed by downsizing with a tip-type sonicator.

The particle size, polydispersity index, and ζ-potential of the resulting liposomes were determined (Zetasizer Nano ZS, Malvern Instruments, Malvern, Worcestershire, United Kingdom). Dynamic light scattering and Laser Doppler velocimetry were performed at 25 °C using a Zetasizer Nano-ZS instrument equipped with Zetasizer Software v.6.01 (Malvern Instruments, Malvern, UK). The polydispersity indices of the liposomes were calculated using the software from the liposome distributions. To calculate the ζ-potential, the Smoluchowski approximation was applied because the liposome radius is much larger than the thickness of a diffuse electric double layer. Measurements were done in triplicate for each sample. Phosphate buffered saline (PBS) was used for liposome measurement.

2.3. Measurement of internalized liposomes

The internalization of liposomes into cells was measured using a protocol published in our previous report (Sakai-Kato et al., 2017). First, HepG2 cells (5×10^5 per well) were seeded into 12-well plates in DMEM containing 10% FBS (1 mL per well). After incubation for 48 h (37 °C, 5% CO_2), liposomes suspended in 500 μL of DMEM containing 10% FBS were added to the cells (final lipid concentration around 50 μg/mL; adjusted to ensure that all liposome solutions of the same compositions had equal fluorescent intensity before administration to cells). The cells were then incubated for a further 2 h (37 °C, 5% CO_2). In the case of DOPC/DOTAP liposomes, the final concentration that was administered was lower than other liposomes at around 20 μg/mL (adjusted to ensure all liposome solutions had equal fluorescent intensity), because the fluorescence intensity of internalized DOPC/DOTAP liposomes 2 h after administration was higher than that of other liposomes. After incubation, the medium was aspirated and replaced with fresh PBS. Cells were trypsinized with 0.25% (v/v) trypsin–EDTA (Life Technologies), washed with Hank's Balanced Salt Solution (HBSS) three times, and suspended in lysis buffer (1.0% [v/v] Triton X-100 in HBSS). The resulting cell suspension was sonicated for 10 min in a bath sonicator, vortexed for 5 min, and centrifuged (15,000 × *g*, 4 °C, 10 min).

The fluorescence intensity of the supernatant was measured with a fluorescence spectrophotometer (F-7000, Hitachi High-Technologies, Tokyo, Japan). The excitation and emission wavelengths were 496 nm and 522 nm respectively for CF-labeled liposomes, and 490 and 540 nm respectively for NBD-labeled liposomes. The background was obtained from the data of cells where no liposomes were administered, and the background values were subtracted from the fluorescence intensity that was measured 2 h after liposome administration. The fluorescence values were also normalized to the protein content of the cell lysate (Protein Assay Kit, Bio-Rad Laboratories, Hercules, CA, USA).

2.4. Statistical analysis

Data were expressed as mean ± S.D. Results were analyzed by multiple comparison analysis using one-way analysis of variance (ANOVA) with Bonferroni's post-hoc test. Differences were considered statistically significant at $P < 0.05$.

3. Results and discussion

3.1. Physicochemical properties of the liposomes

The mean particle sizes and diffusion coefficients of the liposomes are shown in Tables 1–4. The polydispersity indices are also shown in Table 1–4, which were below 0.25 for all liposome preparations. The ζ-potential of DOPC/DOTAP liposomes indicated that the particles were highly positive charged (Table 4), while the other liposomes carried a slight negative charge. (Tables 1–3).

3.2. Size-dependent internalization of liposomes

When HSPC/PEG2000-DSPE/Chol liposomes that were fluorescently labeled with NBD-Chol were administered to HepG2 cells (size range around 87–222 nm; Fig. 1a), the fluorescent intensities were not drastically affected by liposome size. However, the fluorescence intensity observed when liposomes with a diameter of 107 nm were administered was significantly higher than that of liposomes with diameters of 222, 154, 131, 96, or 87 nm (Fig. 1a). This result is in line with those recorded for CF-labeled HSPC/PEG2000-DSPE/Chol liposomes (Fig. 1b). The CF label is carried on the PEG2000-DSPE lipid,

Table 1
Hydrodynamic diameters and zeta potentials of HSPC/PEG2000-DSPE/Chol liposomes. All values are means ± standard deviation ($n = 3$). Values in brackets are % mol. HSPC, hydrogenated soy phosphatidylcholine; PEG2000-DSPE, *N*-(carbonyl-methoxyPEG 2000)-1,2-distearoyl-*sn*-glycero-3-phosphoethanolamine; Chol, cholesterol; NBD-Chol, 25-[*N*-[(7-nitro-2-1,3-benzoxadiazol-4-yl)methyl]amino]-27-norcholesterol; PEG2000-PE-CF, 1,2-distearoyl-sn-glycero-3-phosphoethanolamine-*N*-[poly(ethylene glycol)2000-N′-carboxyfluorescein] (ammonium salt).

Lipid composition	Diameter (nm)	Diffusion Coefficient ($\mu m^2/s$)	Polydispersity index	Zeta potential (mV)
HSPC/DSPE2000-PEG/Chol/NBD-Chol (56.3/5.3/38.4/1)	222 ± 4.5	2.2 ± 0.043	0.19 ± 0.013	−4.4 ± 0.0058
HSPC/DSPE2000-PEG/Chol/NBD-Chol (56.3/5.3/38.4/1)	154 ± 2.6	3.2 ± 0.050	0.049 ± 0.024	−2.3 ± 0.48
HSPC/DSPE2000-PEG/Chol/NBD-Chol (56.3/5.3/38.4/1)	131 ± 3.5	3.8 ± 0.10	0.056 ± 0.014	−2.6 ± 0.452
HSPC/DSPE2000-PEG/Chol/NBD-Chol (56.3/5.3/38.4/1)	115 ± 2.9	4.3 ± 0.11	0.080 ± 0.019	−2.5 ± 1.40
HSPC/DSPE2000-PEG/Chol/NBD-Chol (56.3/5.3/38.4/1)	107 ± 2.3	4.6 ± 0.10	0.087 ± 0.016	−2.5 ± 0.17
HSPC/DSPE2000-PEG/Chol/NBD-Chol (56.3/5.3/38.4/1)	96 ± 2.5	5.1 ± 0.13	0.10 ± 0.007	−2.7 ± 0.74
HSPC/DSPE2000-PEG/Chol/NBD-Chol (56.3/5.3/38.4/1)	87 ± 2.2	5.6 ± 0.14	0.12 ± 0.028	−2.9 ± 0.66
HSPC/PEG2000-DSPE/Chol/PEG2000-PE-CF (56.3/4.3/38.4/1)	232 ± 6.3	2.1 ± 0.060	0.21 ± 0.012	−4.6 ± 0.44
HSPC/PEG2000-DSPE/Chol/PEG2000-PE-CF (56.3/4.3/38.4/1)	156 ± 1.8	3.2 ± 0.037	0.044 ± 0.006	−3.9 ± 0.57
HSPC/PEG2000-DSPE/Chol/PEG2000-PE-CF (56.3/4.3/38.4/1)	123 ± 3.0	4.0 ± 0.10	0.037 ± 0.009	−4.0 ± 0.81
HSPC/PEG2000-DSPE/Chol/PEG2000-PE-CF (56.3/4.3/38.4/1)	107 ± 1.1	4.6 ± 0.045	0.21 ± 0.011	−4.1 ± 0.76
HSPC/PEG2000-DSPE/Chol/PEG2000-PE-CF (56.3/4.3/38.4/1)	82 ± 1.5	6.0 ± 0.11	0.025 ± 0.012	−3.2 ± 0.41

while NBD-Chol is a fluorescent analog of cholesterol. This confirms that the fluorescent label does not affect the size dependence of cellular internalization of HSPC/PEG2000-DSPE/Chol liposomes. Although the liposomes have a certain amount of size distribution and rigorous comparison of close sizes might be difficult, the differences in the cellular internalization of liposomes were observed depending on the mean particle sizes.

Next, we examined the size dependence of internalization of HSPC/PEG2000-DSPE liposomes that did not contain cholesterol, which is important for liposomal stability (Pattni et al., 2015). The composition was otherwise the same as that of HSPC/PEG2000-DSPE/Chol liposomes described above. Although the fluorescence intensities did not differ drastically depending on liposome size, liposomes with a diameter of 115 nm showed significantly higher cellular internalization than liposomes with diameters of 201, 181, or 139 nm (Fig. 2a). These results are in line with previous studies that report the cellular internalization of 108 nm HSPC/PEG2000-DSPE/Chol and 106 nm HSPC/PEG2000-DSPE liposomes to be similar (Takechi-Haraya et al., 2017).

Finally, we examined the internalization of HSPC/Chol liposomes without PEG2000-DSPE, which is often included in the composition of long-circulation liposomes (Moghimi et al., 2001). Because of the difficulties in preparing monodisperse 200 nm liposomes, HSPC/Chol liposome samples were prepared with a maximum diameter of 160 nm. The internalization of HSPC/Chol liposomes did not show obvious size dependence, but the fluorescence intensity was significantly greater for 132 nm liposomes than for liposomes with diameters of 143, 103, or 86 nm (Fig. 2b). This is in line with the results of HSPC/PEG2000-DSPE/Chol liposomes, indicating that this inclusion of PEG2000-DSPE does not influence the size dependence of cellular internalization of HSPC /Chol liposomes. This result also agrees with previous studies which have suggested that the internalization of 107 nm HSPC/Chol liposomes is similar to that of HSPC/PEG2000-DSPE/Chol and HSPC/PEG2000-DSPE liposomes of equivalent size (Takechi-Haraya et al., 2017). It has been reported that the rigidity of liposomes affects the efficiency of their internalization (Zhang et al., 2015; Takechi-Haraya et al., 2017; Moghimi et al., 2001; Yi et al., 2011). According to our previous investigations, HSPC/PEG2000-DSPE/Chol liposomes and HSPC/Chol liposomes have similar rigidity, while HSPC/PEG2000-DSPE liposomes are more rigid (Takechi-Haraya et al., 2017). The results of the present study indicate that membrane rigidity does not affect the size dependence of cellular internalization for these three liposomes.

Because the charges of HSPC/PEG2000-DSPE/Chol, HSPC/PEG2000-DSPE, and HSPC/Chol liposomes were all slightly negative (Tables 1–3), we prepared cationic liposomes using DOTAP to assess the influence of surface charge. This lipid is often used in liposomal carriers for the internalization of nucleotides such as DNA and siRNA, which are unstable in blood (Nie et al., 2012; Gjetting et al., 2010; Nogueira et al., 2015; Majzoub et al., 2016). In the case of DOPC/DOTAP liposomes, the concentration of administered liposomes was lower than other liposomes at around 20 μg/mL (adjusted to ensure all liposome solutions had equal fluorescence intensity). This was because the fluorescence intensity of internalized DOPC/DOTAP liposomes 2 h after administration was higher than that of other liposomes (data not shown). As can be seen in Fig. 2c, maximum internalization was observed when the liposomes had a diameter of 178 nm, which was significantly higher

Table 2
Hydrodynamic diameters and zeta potentials of HSPC/PEG2000-DSPE liposomes. All values are means ± standard deviation ($n = 3$). Values in brackets are %mol. HSPC, hydrogenated soy phosphatidylcholine; PEG2000-DSPE, *N*-(carbonyl-methoxyPEG 2000)-1,2-distearoyl-*sn*-glycero-3-phosphoethanolamine; NBD-Chol, 25-[*N*-[(7-nitro-2-1,3-benzoxadiazol-4-yl)methyl]amino]-27-norcholesterol.

Lipid composition	Diameter (nm)	Diffusion Coefficient ($\mu m^2/s$)	Polydispersity index	Zeta potential (mV)
HSPC/PEG2000-DSPE/NBD-Chol (94.7/5.3/1)	201 ± 1.5	2.5 ± 0.020	0.17 ± 0.014	−2.2 ± 0.29
HSPC/PEG2000-DSPE/NBD-Chol (94.7/5.3/1)	181 ± 1.2	2.7 ± 0.020	0.17 ± 0.014	−2.6 ± 1.6
HSPC/PEG2000-DSPE/NBD-Chol (94.7/5.3/1)	139 ± 1.3	3.5 ± 0.030	0.092 ± 0.012	−3.3 ± 0.89
HSPC/PEG2000-DSPE/NBD-Chol (94.7/5.3/1)	131 ± 2.7	3.8 ± 0.077	0.11 ± 0.013	−2.8 ± 0.25
HSPC/PEG2000-DSPE/NBD-Chol (94.7/5.3/1)	115 ± 1.2	4.3 ± 0.040	0.14 ± 0.005	−2.5 ± 0.36
HSPC/PEG2000-DSPE/NBD-Chol (94.7/5.3/1)	94 ± 0.95	5.3 ± 0.055	0.20 ± 0.004	−2.3 ± 0.085

Table 3
Hydrodynamic diameters and zeta potentials of HSPC/Chol liposomes. All values are means ± standard deviation (n = 3). Values in brackets are %mol. HSPC, hydrogenated soy phosphatidylcholine; Chol, cholesterol; NBD-Chol, 25-[*N*-[(7-nitro-2-1,3-benzoxadiazol-4-yl)methyl]amino]-27-norcholesterol.

Lipid composition	Diameter (nm)	Diffusion Coefficient ($\mu m^2/s$)	Polydispersity index	Zeta potential (mV)
HSPC/Chol/NBD-Chol (60/39/1)	160 ± 2.1	3.1 ± 0.041	0.093 ± 0.006	−2.5 ± 0.079
HSPC/Chol/NBD-Chol (60/39/1)	143 ± 0.61	3.4 ± 0.011	0.14 ± 0.006	−3.8 ± 0.31
HSPC/Chol/NBD-Chol (60/39/1)	132 ± 0.93	3.8 ± 0.026	0.12 ± 0.012	−4.0 ± 0.23
HSPC/Chol/NBD-Chol (60/39/1)	123 ± 0.84	4.0 ± 0.028	0.18 ± 0.007	−4.2 ± 0.19
HSPC/Chol/NBD-Chol (60/39/1)	112 ± 1.4	4.4 ± 0.051	0.18 ± 0.003	−4.2 ± 0.88
HSPC/Chol/NBD-Chol (60/39/1)	103 ± 1.0	4.8 ± 0.050	0.20 ± 0.008	−4.1 ± 0.73
HSPC/Chol/NBD-Chol (60/39/1)	86 ± 1.2	5.8 ± 0.083	0.11 ± 0.012	−4.2 ± 0.85

than all other sized liposomes. The fluorescence intensity of this population was six-fold higher than that of the population which showed the lowest cellular internalization (DOPC/DOTAP liposomes of 89 nm diameter). This is a much greater difference to that seen for the three anionic liposome preparations, where the internalization depending varied less than two-fold between different sized populations. These results confirm that surface charge influences the size dependence of internalization of liposomes.

Several mechanisms are known for the incorporation of nanoparticles into cells. These include endocytosis, phagocytosis, macropinocytosis, clathrin-mediated endocytosis, caveolae-dependent endocytosis, clathrin- and caveolae-independent endocytosis (ligand–receptor binding), nonspecific incorporation, and translocation (Sahay et al., 2010; Zhang et al., 2015). In the case of cationic liposomes, DOPC/DOTAP liposomes have been reported to be internalized mainly through clathrin-mediated endocytosis (Un et al., 2014) or through both clathrin- and caveolae-mediated endocytosis (Pozzi et al., 2014; Sarker et al., 2014; Cui et al., 2014).

When nanoparticles including liposomes are internalized a highly heterogeneous nanoparticle–cell interface is formed, and a dynamic interaction is initiated. Different forces contribute to the interaction, which modify the associated energy balance and therefore dictate the mode of internalization of the nanoparticles (Zhang et al., 2015). First, energy is required to envelope the nanoparticles forces curvature of the cell membrane, which works against membrane tension and resists endocytosis. Opposing forces including electrostatic, van der Waals, hydrophobic, and ligand–receptor binding forces work together to produce an adhesion energy, which drives endocytosis (Zhang et al., 2015). It is reported that balancing the adhesion and membrane deformation energies defines the lower limit of the nanoparticle radius when nonspecific adhesion is the only driving force for membrane wrapping (Zhang et al., 2015). On the other hand, when specific interactions such as ligand–receptor binding occur, the ligand number also affect the upper and lower nanoparticle size limits of endocytosis (Yuan and Zhang, 2010).

Because the plasma membrane is negatively charged, we hypothesize that a strong interaction occurs between DOPC/DOTAP liposomes

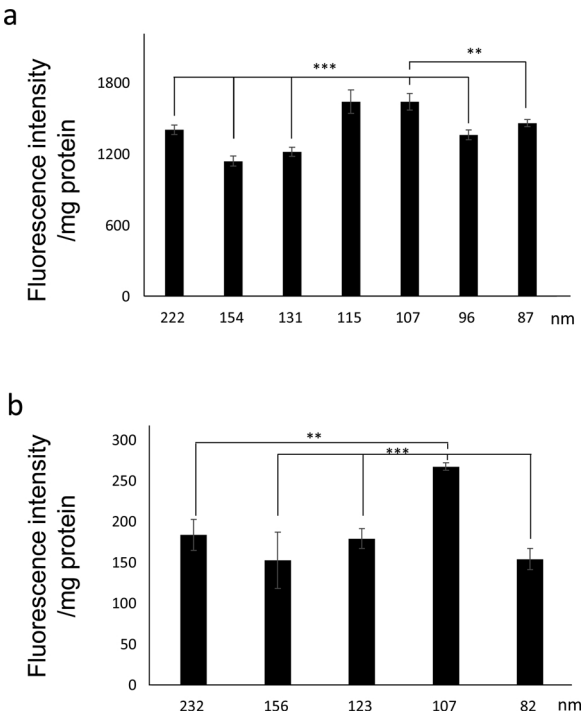

Fig. 1. Effect of liposomal size on the internalization of HSPC/PEG2000-DSPE/Chol liposomes into HepG2 cells. Fluorescence was evaluated 2 h after labeled liposomes were added to HepG2 cells. (a) Liposomes were composed of lipids, PEGylated lipids, cholesterol, and fluorescently labeled cholesterol (NBD-Chol). All values are means ± standard deviation (n = 3). $^{**}P < 0.01$, and $^{***}P < 0.001$, compared with liposomes with a diameter of 107 nm. (b) Liposomes were composed of lipids, PEGylated lipids, fluorescently labeled PEGylated lipids (PEG-CF), and cholesterol. All values are means ± standard deviation (n = 3). $^{**}P < 0.01$, and $^{***}P < 0.001$, compared with liposomes with a diameter of 107 nm.

Table 4
Hydrodynamic diameters and zeta potentials of DOPC/DOTAP liposomes. All values are means ± standard deviation (n = 3). Values in brackets are %mol. DOPC, 1,2-dioleoyl-*sn*-glycero-3-phosphocholine; DOTAP, 1,2-dioleoyl-3-trimethylammoniumpropane; NBD-DOPC, 1-Oleoyl-2-[12-[(7-nitro-2-1,3-benzoxadiazol-4-yl)amino]dodecanoyl]-sn-Glycero-3-Phosphocholine.

Lipid composition	Diameter (nm)	Diffusion Coefficient ($\mu m^2/s$)	Polydispersity index	Zeta potential (mV)
DOPC/DOTAP/NBD-DOPC (49/50/1)	223 ± 1.4	2.2 ± 0.017	0.21 ± 0.012	31 ± 1.5
DOPC/DOTAP/NBD-DOPC (49/50/1)	178 ± 0.75	2.3 ± 0.012	0.16 ± 0.010	28 ± 1.3
DOPC/DOTAP/NBD-DOPC (49/50/1)	138 ± 1.0	3.6 ± 0.029	0.22 ± 0.009	29 ± 1.9
DOPC/DOTAP/NBD-DOPC (49/50/1)	133 ± 0.79	3.7 ± 0.021	0.22 ± 0.008	28 ± 0.76
DOPC/DOTAP/NBD-DOPC (49/50/1)	117 ± 0.75	4.2 ± 0.029	0.22 ± 0.024	30 ± 1.6
DOPC/DOTAP/NBD-DOPC (49/50/1)	89 ± 0.16	5.5 ± 0.012	0.25 ± 0.011	26 ± 0.38

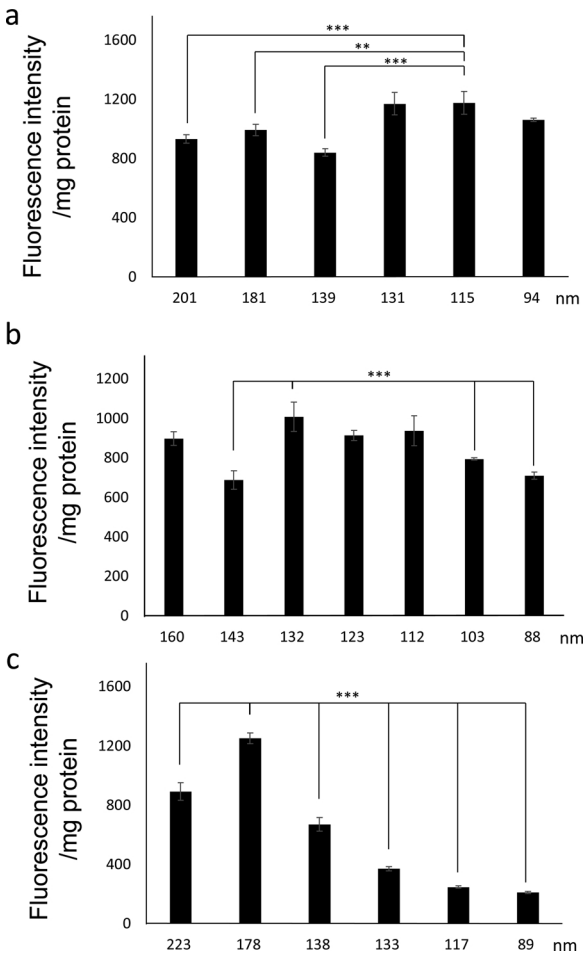

Fig. 2. Effect of liposomal size on the internalization of HSPC/PEG2000-DSPE liposomes (a), HSPC/Chol liposomes (b), and DOPC/DOTAP liposomes (c) into HepG2 cells. Fluorescence was evaluated 2 h after labeled liposomes were added to HepG2 cells. Data are presented as means ± standard deviation ($n = 3$). All values are means ± standard deviation (n = 3). $^{**}P < 0.01$, and $^{***}P < 0.001$, compared with liposomes with a diameter of (a)115 nm, (b) 132 nm, and (c) 178 nm.

and the plasma membrane, resulting in an associated energy balance significantly different from those of the other liposomes used in this study. This therefore causes differences in the size-dependent internalization of the liposome species.

4. Conclusions

The present study reports that size dependence of liposome internalization is significantly affected by the surface charge of the liposomes. Cationic liposomes are internalized at increased sizes compared with other liposomes and are very sensitive to size changes, exhibiting large variations in internalization depending on liposome diameter. Optimization of liposomal formulations is typically carried out by trialing various lipid compositions using a fixed particle size of around 100 nm. However, our results show that examining the size-dependent internalization of each liposome formulation is critical. This is important for maximizing the efficacy of the drugs within the liposomes, minimizing safety concerns, and for determining the optimal size range of the liposomal carriers for quality control.

Acknowledgements

This work was supported in part by a JSPS KAKENHI (grant no. 15K07915 [K.S.-K.]) and by funding for Research on Regulatory Harmonization and Evaluation of Pharmaceuticals, Medical Devices, Regenerative and Cellular Therapy Products, Gene Therapy Products, and Cosmetics from the Japan Agency for Medical Research and Development, AMED (grant no. 18mk0101082j0102). The authors would like to thank R. Takizawa and T. Mano for their technical assistance with the experiments.

References

Ahlbach, C.L., Lexa, K.W., Bockus, A.T., Chen, V., Crews, P., Jacobson, M.P., Lokey, R.S., 2015. Beyond cyclosporine A: conformation-dependent passive membrane permeabilities of cyclic peptide natural products. Future Med. Chem. 7, 2121–2130. https://doi.org/10.4155/fmc.15.78.

Bangham, A.D., Standish, M.M., Watkins, J.C., 1965. Diffusion of univalent ions across the lamellae of swollen phospholipids. J. Mol. Biol. 13, 238–252. https://doi.org/10.1016/S0022-2836(65)80093-6.

Barenholz, Y., 2012. Doxil®–the first FDA-approved nano-drug: lessons learned. J. Control. Release 160, 117–134. https://doi.org/10.1016/j.jconrel.2012.03.020.

Cui, S., Wang, B., Zhao, Y., Chen, H., Ding, H., Zhi, D., Zhang, S., 2014. Transmembrane routes of cationic liposome-mediated gene delivery using human throat epidermis cancer cells. Biotechnol. Lett. 36, 1–7. https://doi.org/10.1007/s10529-013-1325-0.

Dowdy, S.F., 2017. Overcoming cellular barriers for RNA therapeutics. Nat. Biotechnol. 35, 222–229. https://doi.org/10.1038/nbt.3802.

Ehmann, F., Sakai-Kato, K., Duncan, R., Pérez de la, Hernán, Ossa, D., Pita, R., Vidal, J.M., Kohli, A., Tothfalusi, L., Sanh, A., Tinton, S., Robert, J.L., Silva Lima, B., Amati, M.P., 2013. Next-generation nanomedicines and nanosimilars: EU regulators' initiatives relating to the development and evaluation of nanomedicines. Nanomedicine (Lond.) 8, 849–856. https://doi.org/10.2217/nnm.13.68.

Ferrari, M., 2005. Cancer nanotechnology: opportunities and challenges. Nat. Rev. Cancer 5, 161–171. https://doi.org/10.1038/nrc1566.

Gjetting, T., Arildsen, N.S., Christensen, C.L., Poulsen, T.T., Roth, J.A., Handlos, V.N., Poulsen, H.S., 2010. In vitro and in vivo effects of polyethylene glycol (PEG)-modified lipid in DOTAP/Cholesterol-mediated gene transfection. Int. J. Nanomed. 5, 371–383.

Khvorova, A., Watts, J.K., 2017. The chemical evolution of oligonucleotide therapies of clinical utility. Nat. Biotechnol. 35, 238–248. https://doi.org/10.1038/nbt.3765.

Majzoub, R.N., Wonder, E., Ewert, K.K., Kotamraju, V.R., Teesalu, T., Safinya, C.R., 2016. Rab11 and lysotracker markers reveal correlation between endosomal pathways and transfection efficiency of surface-functionalized cationic liposome-DNA nanoparticles. J. Phys. Chem. B 120, 6439–6453. https://doi.org/10.1021/acs.jpcb.6b04441.

Moghimi, S.M., Hunter, A.C., Murray, J.C., 2001. Long-circulating and target-specific nanoparticles: theory to practice. Pharmacol. Rev. 53, 283–318 10.1.1.130.4769.

Nie, Y., Ji, L., Ding, H., Xie, L., Li, L., He, B., Wu, Y., Gu, Z., 2012. Cholesterol derivatives based charged liposomes for doxorubicin delivery: preparation, in vitro and in vivo characterization. Theranostics 2, 1092–1103. https://doi.org/10.7150/thno.4949.

Nogueira, E., Gomes, A.C., Preto, A., Cavaco-Paulo, A., 2015. Design of liposomal formulations for cell targeting. Colloids Surf. B Biointerfaces 136, 514–526. https://doi.org/10.1016/j.colsurfb.2015.09.034.

Pattni, B.S., Chupin, V.V., Torchilin, V.P., 2015. New developments in liposomal drug delivery. Chem. Rev. 115, 10938–10966. https://doi.org/10.1021/acs.chemrev.5b00046.

Pozzi, D., Marchini, C., Cardarelli, F., Salomone, F., Coppola, S., Montani, M., Zabaleta, M.E., Digman, M.A., Gratton, E., Colapicchioni, V., Caracciolo, G., 2014. Mechanistic evaluation of the transfection barriers involved in lipid-mediated gene delivery: interplay between nanostructure and composition. Biochim. Biophys. Acta 1838, 957–967. https://doi.org/10.1016/j.bbamem.2013.11.014.

Sahay, G., Alakhova, D.Y., Kabanov, A.V., 2010. Endocytosis of nanomedicines. J. Control. Release 145, 182–195. https://doi.org/10.1016/j.jconrel.2010.01.036.

Sakai-Kato, K., Nishiyama, N., Kozaki, M., Nakanishi, T., Matsuda, Y., Hirano, M., Hanada, H., Hisada, S., Onodera, H., Harashima, H., Matsumura, Y., Kataoka, K., Goda, Y., Okuda, H., Kawanishi, T., 2015. General considerations regarding the in vitro and in vivo properties of block copolymer micelle products and their evaluation. J. Control. Release 210, 76–83. https://doi.org/10.1016/j.jconrel.2015.05.259.

Sakai-Kato, K., Sakurai, M., Takechi-Haraya, Y., Nanjo, K., Goda, Y., 2017. Involvement of scavenger receptor class B type 1 and low-density lipoprotein receptor in the internalization of liposomes into HepG2 cells. Biochim. Biophys. Acta 1859, 2253–2258. https://doi.org/10.1016/j.bbamem.2017.09.005.

Sarker, S.R., Hokama, R., Takeoka, S., 2014. Intracellular delivery of universal proteins using a lysine headgroup containing cationic liposomes: deciphering the uptake mechanism. Mol. Pharm. 11, 164–174. https://doi.org/10.1021/mp400363z.

Takechi-Haraya, Y., Goda, Y., Sakai-Kato, K., 2017. Control of liposomal penetration into three-dimensional multicellular tumor spheroids by modulating liposomal membrane rigidity. Mol. Pharm. 14, 2158–2165. https://doi.org/10.1021/acs.molpharmaceut.7b00051.

Uhlén, M., Fagerberg, L., Hallström, B.M., Lindskog, C., Oksvold, P., Mardinoglu, A., Sivertsson, Å., Kampf, C., Sjöstedt, E., Asplund, A., Olsson, I., Edlund, K., Lundberg, E., Navani, S., Szigyarto, C.A., Odeberg, J., Djureinovic, D., Takanen, J.O., Hober, S., Alm, T., Edqvist, P.H., Berling, H., Tegel, H., Mulder, J., Rockberg, J., Nilsson, P., Schwenk, J.M., Hamsten, M., von Feilitzen, K., Forsberg, M., Persson, L., Johansson, F., Zwahlen, M., von Heijne, G., Nielsen, J., Pontén, F., 2015. Proteomics. Tissue-based map of the human proteome. Science 347, 1260419. https://doi.org/10.1126/

science.1260419.
Un, K., Sakai-Kato, K., Goda, Y., 2014. Intracellular trafficking mechanism of cationic phospholipids including cationic liposomes in HeLa cells. Pharmazie 69, 525–531. https://doi.org/10.1691/ph.2014.3230.
Yi, X., Shi, X., Gao, H., 2011. Cellular uptake of elastic nanoparticles. Phys. Rev. Lett. 107, 098101. https://doi.org/10.1103/PhysRevLett.107.098101.
Yuan, H., Zhang, S., 2010. Effects of particle size and ligand density on the kinetics of receptor-mediated endocytosis of nanoparticles. Appl. Phys. Lett. 96, 033704. https://doi.org/10.1063/1.3293303.
Zhang, S., Gao, H., Bao, G., 2015. Physical principles of nanoparticle cellular endocytosis. ACS Nano 9, 8655–8671. https://doi.org/10.1021/acsnano.5b03184.